Tuning the properties of exciton complexes in self-assembled GaSb/GaAs quantum rings

M. Ahmad Kamarudin,[1,2] M. Hayne,[1,*] R. J. Young,[1] Q. D. Zhuang,[1] T. Ben,[3] and S. I. Molina[3]

[1]*Department of Physics, Lancaster University, Lancaster LA1 4YB, United Kingdom*

[2]*Department of Physics, Faculty of Science, Universiti Putra Malaysia, 43400 UPM Serdang, Selangor Darul Ehsan, Malaysia*

[3]*Departamento de Ciencia de los Materiales e I. M. y Q. I., Facultad de Ciencias, Universidad de Cádiz, Campus Río San Pedro, s/n, Puerto Real, Cádiz 11510, Spain*

(Received 21 October 2010; revised manuscript received 4 January 2011; published 10 March 2011)

Type-II self-assembled GaSb/GaAs nanostructures have been grown by molecular-beam epitaxy and studied by atomic-force microscopy, transmission electron microscopy, and power-dependent magnetophotoluminescence. Nanostructures on the sample surface are found to be entirely dotlike, while capped nanostructures are predominantly ringlike. Moreover, an *in situ* anneal process applied after thinly capping the dots is shown to enhance the severity of the rings and relax the strain in the matrix in the proximity of the GaSb, resulting in a change to the spatial configuration of the exciton complexes and their optical properties.

DOI: 10.1103/PhysRevB.83.115311 PACS number(s): 81.07.Ta, 78.67.Hc, 78.55.Cr, 68.37.Lp

I. INTRODUCTION

Type-II self-assembled nanostructures, which confine either electrons or holes, are fundamentally different from their type-I counterparts. The excitonic properties of type-I quantum dots are determined by the confinement of carriers, whereas for type-II dots it is the Coulomb interaction between confined and free carriers that dominates the physics. The result is that type-II dots exhibit phenomena that are absent in type-I dots, such as Mott transitions[1] and the formation of excitonic helium.[2] In particular, the strongly staggered band alignment of GaSb/(Al)GaAs type-II nanostructures has attracted much interest for its potential to extend the absorption spectrum of GaAs solar cells beyond 1 μm,[3] and provide deep confining potentials capable of room-temperature charge storage for memory applications.[4,5] Intriguingly, Timm *et al.* have recently demonstrated that, in stark contrast to GaSb quantum dots grown by metal-organic chemical vapor deposition (MOCVD),[6] capped GaSb nanostructures grown by molecular-beam epitaxy (MBE) tend to form quantum rings (QR's).[7,8] Here, we report results that not only verify these observations, but also show that the morphological properties of the QR's can be modified by changes in the growth procedure, and that these can have strong effects on the associated properties of the excitons and exciton complexes they confine. This dramatically improves the prospects for tailoring the electronic properties of GaSb/GaAs self-assembled nanostructures for the observation of particular phenomena, e.g., Aharonov-Bohm (AB) oscillations,[9] and for device applications.[3–5] The remainder of the paper is organized as follows. In Sec. II, we briefly outline the growth procedure of the samples. Section III describes microscopy measurements using atomic-force microscopy (AFM) and transmission electron microscopy (TEM). Section IV describes power-dependent magnetophotoluminescence (PL) data, while Sec. IV discusses the interpretation of the results in terms of the spatial configurations of the excitons in the two samples and the relative strengths of the electron-electron and electron-hole interactions. Finally, Sec. VI contains the conclusions.

II. SAMPLE GROWTH

The samples were grown using solid-source MBE by deposition of a GaAs buffer layer at a pyrometer-measured temperature of 580 °C, followed by the deposition of nominally 2.1 monolayers (ML's) of GaSb at 490 °C, at a rate of 0.3 ML s^{-1} and with a V/III ratio of 2. This was followed by the growth of an ∼9-nm cold-cap of GaAs at 430 °C.[10] The first sample, *A* (no anneal), was then capped further with 100 nm of GaAs grown at 1 ML s^{-1} at a temperature of 500 °C,[11] while a second sample, *B* (anneal), was subjected to a 2-min growth interruption under As_2 flux at 580 °C before being capped with 100 nm of GaAs at the same temperature and a growth rate of 1 ML s^{-1}. A second layer of GaSb was deposited on the surfaces of both samples under the same conditions as the first layer; this was left uncapped to facilitate AFM measurements.

III. MICROSCOPY

Figure 1 shows AFM images taken in tapping mode, using a crystalline Si cantilever and tip. It can be seen that the surface dot morphology is quite different for the two samples. Sample A has larger dots of lower density than sample B (see Table I), most likely a result of the difference in the GaAs grown at different temperatures.[12] However, the point to emphasize here is that in both cases, the surface GaSb nanostructures appear entirely dotlike.

The samples were then studied by cross-sectional TEM in a JEOL 1200EX transmission electron microscope, and high-resolution TEM (HRTEM) and high-angle annular dark field scanning transmission electron microscopy (HAADF-STEM) in a 2010F transmission electron microscope. Figures 2(a) and 2(b) show dark-field TEM images of both samples. HRTEM images of the two types of embedded nanostructures, with single and double lobes, are shown in Figs. 3(a) and 3(b), respectively. Several interesting features are observed. First, the volume of the capped nanostructures is substantially reduced compared to the surface dots;[13] a result of the dissolution effect of capping the nanostructures.[10] Secondly, in both samples, double-lobe features can be seen, indicative of

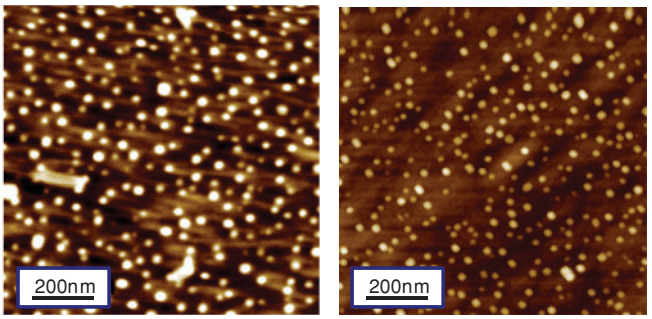

FIG. 1. (Color online) 1 μm $\times$ 1 μm atomic-force-microscopy images of the surfaces of the two samples. Sample A (no anneal) is on the left, and sample B (anneal) is on the right. In both cases, the observed surface nanostructures are entirely dotlike.

the formation of QR's. Remember, no such features were found on the surfaces of these samples (Fig. 1). This is consistent with the report of Timm *et al.*, who presented a statistical analysis of 140 buried GaSb/GaAs nanostructures measured using cross-sectional scanning tunneling microscopy.[6] Even though 69 of them appeared "compact" (single lobe) and 71 as "paired features" (double lobe), they concluded that all the nanostructures were probably QR's. Let us assume a toroidal shape for the QR's with the overall size of the ring defined by radius r_M and the thickness of the ring described by radius r_m. In the case in which $r_m/r_M = 0.5$, taking random cross sections through the rings will generate both paired and compact features with equal probability. Images containing more than 200 nanostructures in the two samples have been analyzed using HAADF-STEM. This revealed that approximately half of the nanostructures in sample A (no anneal) showed a double-lobe cross section, while in sample B (anneal) 75% were doubled-lobed and only 25% single-lobed. It can be inferred from these observations that the growth of a high-temperature GaAs layer subsequent to the initial cold-cap acts to increase the number and/or the severity of the rings, i.e., it reduces the ratio r_m/r_M. The third point of note in Fig. 2 is the presence of shadows that emanate from the GaSb nanostructures in sample A, but are absent in the image of sample B, suggesting enhanced strain in the matrix surrounding the nanostructures in sample A compared with sample B.

TABLE I. Sizes and areal densities of the GaSb QD's on the surfaces of the two samples.

Sample	Lateral size (nm)	Height (nm)	Density (cm^{-2})
A (no anneal)	43 ± 7	2.6 ± 0.8	2.0×10^{10}
B (anneal)	27 ± 6	2.9 ± 0.8	3.2×10^{10}

IV. LOW-TEMPERATURE MAGNETOPHOTOLUMINESCENCE

Finally, low-temperature ($\leqslant$4.2 K) magneto-PL measurements were performed to probe the properties of the excitons confined to the QR's. A frequency-doubled diode-pumped solid-state laser emitting at 532 nm was used to excite the sample, and a 30-cm focal length spectrometer was combined with a Peltier-cooled InGaAs diode array to analyze the luminescence. Optical fibers were used to transmit the light to and from the sample, which was placed in the bore of a superconducting magnet. The laser spot diameter on the sample was $\sim$2 mm, leading to an estimated laser power density of 1 W cm^{-2} with a launch power, P, of 50 mW.

A. Zero-field photoluminescence

Figure 4(a) shows typical zero-field spectra for both samples. They contain features that are characteristic of GaSb/GaAs QD/QR samples (see, for example, Refs. 8,10,14, and 15): narrow peaks at about 1.5 eV correspond to emission from the GaAs matrix, a wetting layer peak at 1.3–1.4 eV, and a peak from the GaSb nanostructures (QR's in this case) at 1.06 eV for sample A and 1.02 eV for sample B. Note that there seems to be no obvious difference in the zero-field PL of GaSb/GaAs QD samples grown by MOVCD[14] and GaSb/GaAs QR samples grown by MBE.[8] There are several potential explanations for the difference in emission energy of the QR's in the two samples: (i) a reduction in QR charging in sample B due to lower unintentional p-doping compared with sample A, (ii) an increase in the size of the

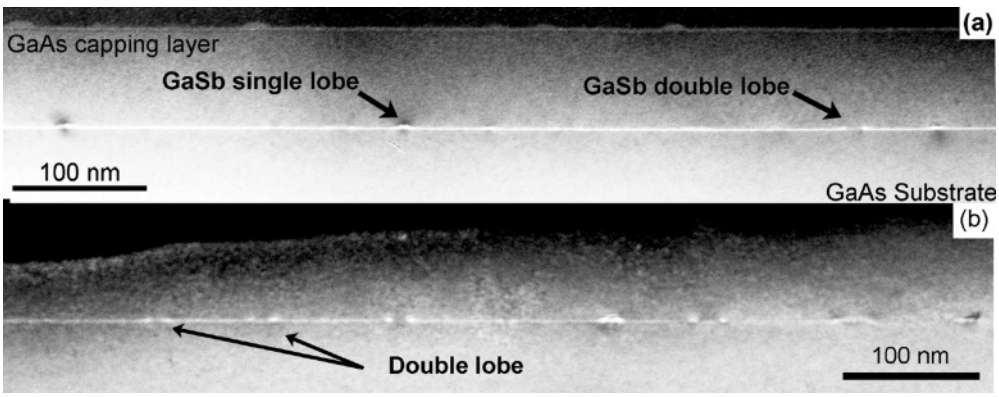

FIG. 2. TEM images of (a) sample A (no anneal) and (b) sample B (anneal) taken in dark-field 002 imaging conditions. In both cases, double-lobed structures can be seen in the images. In sample A, the dark region above the GaSb nanostructures indicates the presence of strain.

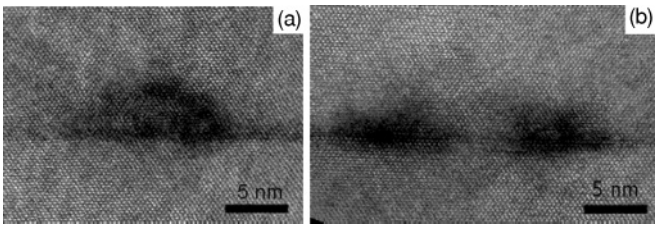

FIG. 3. HRTEM images of a buried single-lobe nanostructure in sample A (a), and a double-lobe nanostructure in sample B (b).

nanostructures in sample B when compared to sample A (thus reducing the quantization energy), or (iii) a change in the composition induced by the different capping conditions for the two samples. Since MBE rather than MOCVD growth was used in this study, strong unintentional doping[16] is not likely. This argument is supported by Fig. 4(b), which plots the change in zero-field energy for the two samples over four orders of magnitude of incident laser power. In both cases, a strong blueshift is seen, a feature that is characteristic of type-II systems and has been observed, for example, in GaSb/GaAs quantum wells,[17] GaSb/GaAs QD's,[1,15,16,18] and InP/GaAs QD's.[2] In the case of type-II quantum wells, it is believed that the shift is the result of band bending at the heterointerface due to charge separation.[17] The same explanation has also been invoked to explain the blueshift in the PL from type-II QD's.[15] However, since QD's exhibit three-dimensional charge confinement, capacitive charging and state-filling effects may also play a role.[18] For MOCVD-grown GaSb/GaAs QD's, it was shown that for sufficiently low laser powers, the blueshift is preceded by a redshift, such that the PL energy traces a U-shaped curve as the laser power is increased.[16] This was attributed to the presence of carbon acceptors that dope the samples such that the dots are fully occupied with holes in the absence of any illumination. A small amount of illumination actually initially discharges the dots in a process known as optically induced density depletion,[19] making the redshift a signature of (unintentional) *p*-doping. Since there is no evidence of a redshift of the QR PL from either sample in Fig. 4(b), we conclude that different levels of unintentional doping cannot explain the difference in PL energy between the two samples. Having said that, it is extremely unlikely that the background carbon doping is zero, and given the deep confining potential of GaSb/GaAs nanostructures,[14] the possibility that the dots are partially occupied (charged) in the absence of illumination cannot be excluded. For this reason, the use of the term "exciton" in this paper should not necessarily be taken to imply single electron-hole pairs, but should be more broadly interpreted to include charged excitons and other exciton complexes. It is important to note that because of the spatial separation of electrons and holes, such exciton complexes in these samples will be fundamentally different from those in type-I systems and are analogous to atoms and ions with electrons bound to a positively charged "nucleus."[2,14]

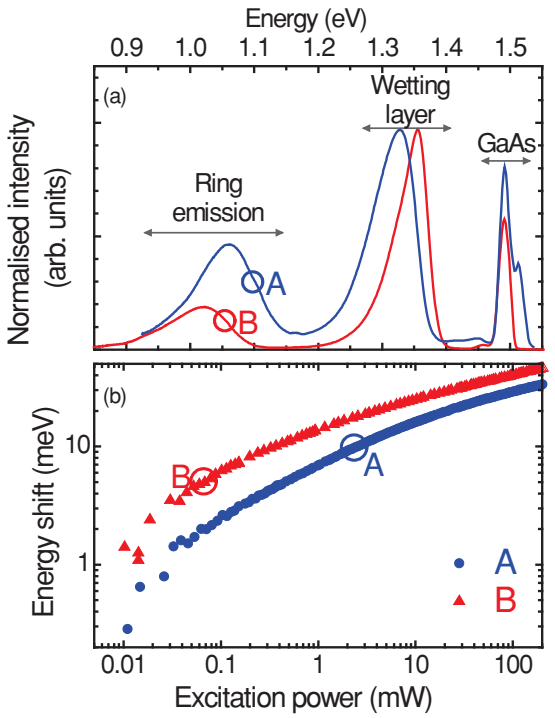

FIG. 4. (Color online) Low-temperature photoluminescence (PL) data at zero magnetic field: sample A (no anneal) is in blue and sample B (anneal) is in red. (a) Spectra: the quantum ring (QR), wetting layer, and GaAs peaks are labeled. (b) Laser-power, *P*, induced blueshift of the QR peak.

The second possible reason for the difference in zero-field PL energy is a change in the hole confinement energies due to a difference in the size of the nanostructures between the two samples. However, confinement energies for holes are much less sensitive to size effects than for electrons, and the TEM data indicate no systematic change in QR base length or height between samples A and B. This leaves only composition as a potential explanation for the observed difference. It is believed that MOCVD-grown GaSb/GaAs QD's have an average composition that is close to $GaAs_{0.4}Sb_{0.6}$,[4] so it could be that the nanostructures in sample B are more pure, leading to a deeper hole localization potential and a correspondingly lower QR PL energy. This is, however, inconsistent with the sample growth; it is sample B that was annealed, and therefore would be expected to have greater intermixing. Instead, we suggest that the lower QR PL energy seen in sample B is associated with lower electron energy due to reduced strain in the GaAs close to the QR's, as evidenced by the TEM images in Fig. 2, combined with an increase in the strength of the excitonic binding, which shall be discussed below.

B. Magnetophotoluminescence

Figure 5 plots the magnetic field, *B*, dependence of the QR PL peak energy for a variety of different laser excitation powers. In addition to the lower PL energy for sample B, some rather striking differences between the two samples now emerge. The first is that the size of the field-induced shift of the PL energy is substantially smaller for sample A than for sample B. This is shown more explicitly in Fig. 6, which plots the total size of shift in the QR PL peak energy from 0 to 15 T as a function of laser power for both samples. To understand the origin of this observation, we compare our data to a model of the field dependence of the PL energy, *E*, in which there

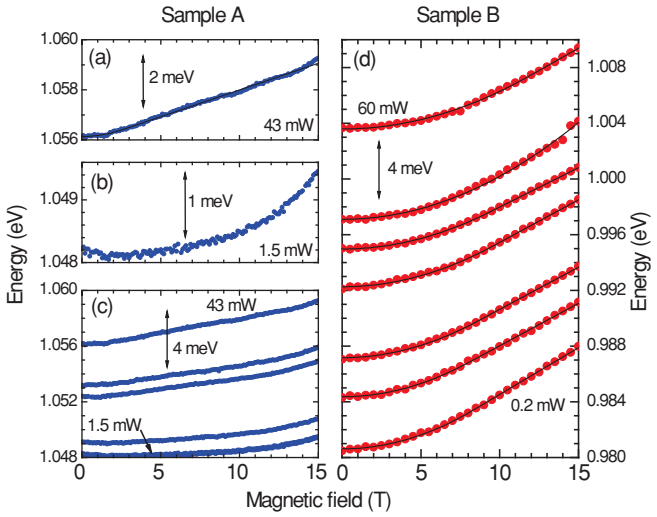

FIG. 5. (Color online) Quantum-ring PL peak position as a function of magnetic field. Sample A (no anneal) is in blue (left-hand panels): (a) high laser power, (b) low laser power, (c) laser power dependence. The right-hand panel (d) shows the laser power dependence for sample B (anneal). The lines are fits to Eqs. (1) and (2). Note that (c) and (d) have the same vertical scale in terms of meV per unit length on the page. It can be seen that the field-induced shift of the PL is much larger for sample B than sample A, and that for sample A the field dependence is highly parabolic at low laser power (b) and more linear at high laser power (a). For sample B, the opposite trend is observed (d).

are two regimes: a low-field regime where the increase in PL energy is proportional to B^2, Ref. 20 and a high-field regime in which the PL energy increases linearly with field.[21] Requiring

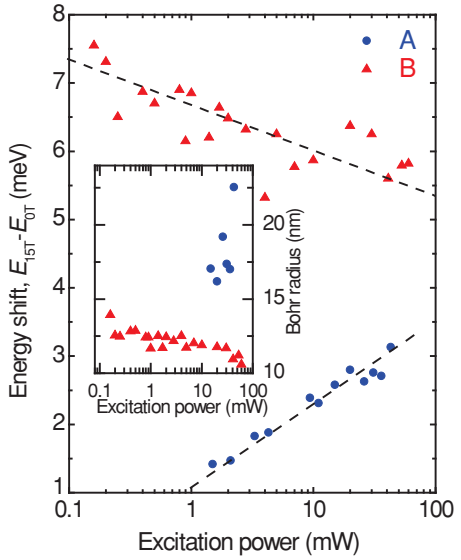

FIG. 6. (Color online) Variation of the magnetic-field, B, induced shift of the QR PL vs laser excitation power, P. Note that an increasing B-shift with increasing laser power indicates increasing excitonic binding with increasing laser power. The lines are guides to the eye. The inset shows the exciton Bohr radius vs P. For sample B (no anneal) and $P < 10$ mW, the Bohr radius is too small to be measured with the magnetic fields available.

a smooth transition between the low- and high-field limits at a critical field, B_c, results in the following expressions:[22,23]

$$E = E_0 + \frac{e^2 a_B^2 B^2}{8\mu} \quad \text{for} \quad B \leqslant B_c \tag{1}$$

and

$$E = E_0 - \frac{\hbar^2}{2\mu a_B^2} + \frac{\hbar e B}{2\mu} \quad \text{for} \quad B \geqslant B_c, \tag{2}$$

where

$$B_c = \frac{2\hbar}{e a_B^2}, \tag{3}$$

E_0 is the zero-field PL energy, $\hbar$ is the reduced Planck constant, e is the electron charge, a_B is the exciton Bohr radius, and μ is the reduced exciton mass.[24] Equations (1) and (2) may be used to determine the useful parameters a_B and μ by fitting the PL peak energy data over the whole field range in a single operation, as can be seen for the data in Fig. 5(d) for sample B. Note that the same analysis was also applied to sample A, but the result cannot easily be seen in Fig. 5 due to the very small size of the shift, even in the enlarged view of the data in Fig. 5(a). An examination of Eqs. (1) and (2) reveals that in both the low- and high-field regimes, the size of the field-induced shift is inversely proportional to μ. Thus, the systematically larger field-induced shift of the PL from sample B implies that μ is lower in this sample, an inference that is consistent with the reduced strain[25] in sample B observed in the TEM images in Fig. 2. The shift of the QR PL for sample A is very small indeed at low laser power, but for powers >10 mW it shows a clear linear field dependence at high fields, giving $\mu = 0.30 \pm 0.02 m_0$ (m_0 is the free-electron mass), while, in contrast, $0.096 \pm 0.005 m_0$ is measured for sample B over the entire power range.

However, the most striking feature of Figs. 5 and 6 is that for sample A, the total size of the field-induced shift of the PL energy *increases* with increasing laser power, whereas for sample B it *decreases* with increasing laser power. Moreover, a close examination of Fig. 5 reveals that the dependence of the PL energy on magnetic field for sample A is parabolic to the highest available fields at low power [Fig. 5(b)], but very quickly becomes linear with field at high power [Fig 5(a)]. For sample B, the opposite trend is observed [Fig. 5(d)]. According to Eq. (3), the transition from parabolic to linear field dependence occurs when the magnetic length is $1/\sqrt{2}$ times the exciton Bohr radius, a_B, and is therefore a measure of the strength of the excitonic binding. Note that stronger excitonic binding (smaller a_B) not only decreases the size of the field-induced shift according to Eq. (1), but it also increases the field at which the linear field dependence is observed. The inset to Fig. 6 shows the Bohr radius derived from the analysis of the data as a function of laser power for the two samples. For sample B, the Bohr radius gradually decreases with increasing power, indicating an increase in excitonic binding, while for sample A, a strong increase in the Bohr radius is observed for laser powers >10 mW, indicating a weakening of the excitonic binding. Given that the Bohr radius is inversely proportional to μ, and that μ for sample A is three times that of sample B, it is quite striking that the Bohr radius for sample B is

larger at high laser power. For excitation powers <10 mW, a_B is so small (<10 nm) that insufficient fields are available to determine its value: the data are characterized by a parabolic field dependence up to the highest fields [Fig. 5(b)].

V. DISCUSSION

In the previous section, we showed that two MBE-grown GaSb QR samples with slightly different growth conditions show opposite dependencies of the excitonic binding on incident laser power. Very similar observations have previously been reported from two different experiments on MOVCD-grown GaSb/GaAs QD's. In one case a decrease in the exciton binding was observed with increasing laser power and attributed to screening of the electrons, ultimately resulting in an insulator-to-metal Mott transition.[1] In the other, exciton binding was found to increase with increasing laser power as a result of charging the dots with additional holes.[14] No explanation for this difference in behavior between the two experiments has been suggested so far. In the present case, well-defined changes in growth conditions and the use of TEM have given insight into subtle changes in the nanostructure morphology, allowing the proposition of an explanation for observed differences in excitonic properties as a result of a change in the spatial configuration of the excitons.

First, we should be reminded of the fundamental difference between type-I and type-II nanostructures. In a type-II QD/QR, only one carrier-type (e.g., hole) can be confined to the volume of the nanostructure; the other (e.g., electron) is free, except for the action of the Coulomb interaction. Hence substantial changes in the spatial configuration of the exciton due to changes in the position and/or wave-function extent of the unconfined carrier are quite likely, and these will be manifested in the optical properties.[1,2] This is not the case in a type-I nanostructure. Given the large valence-band offsets in this system,[14] it can be assumed that in both cases the holes are strongly confined to the GaSb of the QR's. All of the observed excitonic properties can then be explained in terms of the unconfined electrons. Sample A (no anneal) has a smaller opening in the center of the QR than sample B, with a higher Sb content. This exerts tensile strain on the GaAs above the dot, repelling the electron,[14] which is thus weakly bound to the hole. The strained GaAs in sample A also increases the electron effective mass,[25] resulting in a very compact electron wave function, as evidenced by the parabolic form of the field dependence of the QR PL at low laser power. Since the electron is weakly bound to the hole in the QR, when laser power is increased, electron-electron interactions (screening) dominate over electron-hole interactions, resulting in a smearing out of the electron wave function, which *increases* the B-field shift and Bohr radius.[1] Sample B (anneal) has a larger opening in the QR with a lower Sb content. The strain in the GaAs is much lower, reducing the electron effective mass and allowing the electron much closer to the hole: it is possible that it may even sit inside the caldera of the nanovolcano formed by the QR. The lack of strain and the proximity to the hole reduce the PL energy compared to sample A. In this situation, increasing the laser power has quite a different effect; the close proximity of the electron to the QR means that the electron-hole interaction dominates, and as the photoexcited holes charge the QR with increasing laser power, the excitonic binding is increased, not reduced. This *decreases* the size of the B-field shift and the Bohr radius.[14]

Next, we comment on the relative strength of the blueshift of the ($B = 0$) PL energy with increasing laser power, P, for the two samples. In particular, when comparing Figs. 4 and 6, we notice a substantially larger blueshift of the PL energy with increasing laser power for the sample where excitonic binding increases with laser power (sample B). The same trend is observed for MOCVD-grown QD's.[1,14] It was argued in Sec. IV that, given the comparable dimensions of the nanostructures and the heavy mass of the hole, it is unlikely that there is a substantial difference in the confined hole states for the two samples, and that the above difference in PL energy is a result in a change in the electron configuration. Similarly, although state filling could contribute to the blueshift for both samples, it is an improbable explanation for the factor-of-4 difference in the total blueshift between the two samples. If we model a type-II QD as a simple parallel plate capacitor, the capacitive charging energy is proportional to the distance between the plates, i.e., the electron-hole separation. Since the large blueshift is observed in the sample where the electron-hole interaction is dominant, i.e., the electron-hole separation is reduced, this implies that band bending, not capacitive charging, is responsible. Unfortunately, a simple model of capacitive charging gives a $P^{1/2}$ dependence, making it very difficult to distinguish it experimentally from band bending, which gives $P^{1/3}$. This is presently the subject of further investigation.

Finally, we make some brief remarks about the observation of AB oscillations in (self-assembled) semiconductor QR's. Although appealing, observation of the effect in magneto-PL appears to be very difficult. In type-I InGaAs/GaAs QR's, it was shown that the effect is suppressed due to confinement of both electron and hole and the Coulomb interaction between them,[26] i.e., neutral excitons with a ringlike geometry do not undergo AB oscillations. It has, however, been observed in charged type-I rings using magneto-PL (Ref. 27) and magnetization experiments.[28] Any manifestation of the effect seems to be absent from the data reported here. AB oscillations in semiconductor nanostructures can be regarded as transitions to higher angular momentum states, making it a subtle effect in hole-confining rings where the separation between quantum states is very small. This problem will be accentuated by the dominant role that the electron seems to play in determining the excitonic properties. On the other hand, we have shown that it is possible to tune these properties by changing the growth conditions and also the laser excitation power. We therefore hope that this will stimulate further theoretical and experimental work, leading to the observation of AB oscillations in GaSb QR's in the future.

VI. CONCLUSIONS

The properties of MBE-grown GaSb/GaAs nanostructures were investigated. Two samples were grown under the same conditions, except for the higher-temperature growth and anneal of the second sample after the initial cold-cap. In

both cases, only GaSb quantum dots are observed on the surface, whereas the capped nanostructures are predominantly quantum rings, confirming the results of Timm *et al.*[7] *In situ* annealing of the second sample resulted in changes in the ring morphology that effect the spatial configuration of the excitons, leading to quite different optical properties in the two samples: in the no-anneal sample (A), electron-electron interactions dominate, while in the annealed sample (B), electron-hole interactions dominate. This opens up the prospect for control of the electronic properties of GaSb/GaAs self-assembled nanostructures, which will be crucial for the observation of new physics and the development of new devices.

ACKNOWLEDGMENTS

This work was supported by the Engineering and Physical Sciences Research Council (Grant No. EP/H006419) in the framework of the QD2D project, and the Royal Society–Brian Mercer Feasibility Award. M.H. acknowledges support of the Research Councils, UK, and M.A.K. thanks the Ministry of Higher Education, Malaysia. T.B. and S.I.M. acknowledge support from the Spanish MCI (TEC2008-06756-C03-02/TEC and CONSOLIDER INGENIO 2010 CSD2009-00013)) and the Junta de Andalucía (PAI research group TEP-120; project P08-TEP-03516).

*m.hayne@lancaster.ac.uk

[1] B. Bansal, M. Hayne, M. Geller, D. Bimberg, and V. V. Moshchalkov, Phys. Rev. B **77**, 241304(R) (2008).
[2] B. Bansal, S. Godefroo, M. Hayne, G. Medeiros-Ribeiro, and V. V. Moshchalkov, Phys. Rev. B **80**, 205317 (2009).
[3] R. B. Laghumavarapu, A. Moscho, A. Khoshakhlagh, M. El-Emawy, L. F. Lester, and D. L. Huffaker, Appl. Phys. Lett. **90**, 173125 (2009).
[4] A. Marent, M. Geller, A. Schliwa, D. Feise, K. Pötsche, D. Bimberg, N. Akçay, and N. Öncan, Appl. Phys. Lett. **91**, 242109 (2007).
[5] M. Geller, A. Marent, T. Nowozin, D. Bimberg, N. Akçay, and N. Öncan, Appl. Phys. Lett. **92**, 092108 (2008).
[6] R. Timm, H. Eisele, A. Lenz, S. K. Becker, J. Grabowski, T.-Y. Kim, L. Müller-Kirsch, K. Pötsche, U. W. Pohl, D. Bimberg, and M. Dähne, Appl. Phys. Lett. **85**, 5890 (2004).
[7] R. Timm, H. Eisele, A. Lenz, L. Ivanova, G. Balakrishnan, D. L. Huffaker, and M. Dähne, Phys. Rev. Lett. **101**, 256101 (2008).
[8] R. Timm, H. Eisele, A. Lenz, L. Ivanova, V. Vossebürger, T. Warming, D. Bimberg, I. Farrer, D. A. Ritchie, and M. Dähne, Nano Lett. **10**, 3972 (2010).
[9] M. Grochol, F. Grosse, and R. Zimmermann, Phys. Rev. B **74**, 115416 (2006).
[10] M. Ahmad Kamarudin, M. Hayne, Q. D. Zhuang, O. Kolosov, T. Nuytten, V. V. Moshchalkov, and F. Dinelli, J. Phys. D **43**, 065402 (2010).
[11] This sample is the same as sample *F* in Ref. 10. For clarification, it should be noted that the upper GaAs layers of this sample were not deposited at 580 °C, as is implied in Ref. 10.
[12] H. Morales-Cortés, C. Mejía-García, V. H. Méndez-García, D. Vázquez-Cortés, J. S. Rojas-Ramírez, R. Contreras-Guerrero, M. Ramírez-López, I. Martínez-Velis, and M. López-López, Nanotechnology **21**, 134012 (2010).
[13] S. I. Molina, A. M. Beltrán, T. Ben, P. L. Galindo, E. Guerrero, A. G. Taboada, J. M. Ripalda, and M. F. Chisholm, Appl. Phys. Lett. **94**, 043114 (2009).
[14] M. Hayne, J. Maes, S. Bersier, V. V. Moshchalkov, A. Schliwa, L. Müller-Kirsch, C. Kapteyn, R. Heitz, and D. Bimberg, Appl. Phys. Lett. **82**, 4355 (2003).
[15] D. Alonso-Álvarez, B. Alén, J. M. García, and J. M. Ripalda, Appl. Phys. Lett. **91**, 263103 (2007).
[16] M. Hayne, O. Razinkova, S. Bersier, R. Heitz, L. Müller-Kirsch, M. Geller, D. Bimberg, and V. V. Moshchalkov, Phys. Rev. B **70**, 081302(R) (2004).
[17] N. N. Ledentsov, J. Böhrer, M. Beer, F. Heinrichsdorff, M. Grundmann, D. Bimberg, S. V. Ivanov, B. Ya. Meltser, S. V. Shaposhnikov, I. N. Yassievich, N. N. Faleev, P. S. Kop'ev, and Z. I. Alferov, Phys. Rev. B **52**, 14058 (1995).
[18] L. Müller-Kirsch, R. Heitz, A. Schliwa, O. Stier, D. Bimberg, H. Kirmse, and W. Neumann, Appl. Phys. Lett. **78**, 1418 (2001).
[19] M. Hayne, A. Usher, A. S. Plaut, and K. Ploog, Phys. Rev. B **50**, 17208 (1994).
[20] S. N. Walck and T. L. Reinecke, Phys. Rev. B **57**, 9088 (1998).
[21] P. D. Wang, J. L. Merz, S. Fafard, R. Leon, D. Leonard, G. Medeiros-Ribeiro, M. Oestreich, P. M. Petroff, K. Uchida, N. Muira, H. Akiyama, and H. Sakaki, Phys. Rev. B **53**, 16458 (1996).
[22] M. Hayne, R. Provoost, M. K. Zundel, Y. M. Manz, K. Eberl, and V. V. Moshchalkov, Phys. Rev. B **62**, 10324 (2000).
[23] M. Hayne, J. Maes, S. Bersier, M. Henini, L. Müller-Kirsch, R. Heitz, D. Bimberg, and V. V. Moshchalkov, Physica B **346–347**, 421 (2004)
[24] Note that determining the reduced exciton mass by this method neglects any magnetic-field dependence of the binding energy, and therefore gives an upper limit.
[25] C. Pryor, Phys. Rev. B **57**, 7190 (1998).
[26] N. A. J. M. Kleemans, J. H. Blokland, A. G. Taboada, H. C. M. van Genuchten, M. Bozkurt, V. M. Fomin, V. N. Gladilin, D. Granados, J. M. García, P. C. M. Christianen, J. C. Maan, J. T. Devreese, and P. M. Koenraad, Phys. Rev. B **80**, 155318 (2009).
[27] M. Bayer, M. Korkusinski, P. Hawrylak, T. Gutbrod, M. Michel, and A. Forchel, Phys. Rev. Lett. **90**, 186801 (2003).
[28] A. J. M. Kleemans, I. M. A. Bominaar-Silkens, V. M. Fomin, V. N. Gladilin, D. Granados, A. G. Taboada, J. M. García, P. Offermans, U. Zeitler, P. C. M. Christianen, J. C. Maan, J. T. Devreese, and P. M. Koenraad, Phys. Rev. Lett. **99**, 146808 (2007).